Force Behavior in Long-Distance Pipe Jacking across Composite Strata: Field and Numerical Analyses

Shaohui Liu, Liang Xiong*, Li Liu

SINOHYDRO BUREAU 5 Co., LTD, Chengdu, China
*Corresponding authors: Liang Xiong E-mail address: 824949236@qq.com

Abstract. Jacking force is a key parameter in pipe jacking construction. To analyze the mechanical properties of large-diameter reinforced concrete pipe jacking in composite strata, the jacking force, face resistance, circumferential pressure and strain were monitored. And strain was conducted based on the non-pressure cave section of Inner Mongolia water diversion project. Based on the field measurements, the friction coefficient of the pipe jacking through various strata was calculated. A three-dimensional finite element model of the pipe jacking construction was then established using ABAQUS numerical simulation software. The calculated friction coefficient is substituted into the numerical model. Simulated jacking forces are derived from numerical modeling. The measured jacking force, the simulated jacking force and the predicted jacking force based on the prediction model of jacking force proposed by Staheli are compared. Simulated jacking forces align closely with field measurements, outperforming Staheli's predictions. This shows that it is appropriate to substitute the parameters obtained based on the field measured data into the numerical model, yielding high-fidelity results. The proposed prediction method offers a robust benchmark for future pipe-jacking projects.

Keywords: Jacking Force; Numerical Simulation; Field Monitoring Area; Friction Coefficient.

1 Introduction

Pipe jacking is an efficient, safe, and eco-friendly trenchless technique for underground infrastructure [1]. As urbanization increasingly restricts traditional open-cut excavation, pipe jacking is widely adopted for municipal pipelines, utility tunnels, and underground passages due to its minimal surface disruption and rapid execution [2]. A core challenge in this method is predicting and controlling the jacking force. This critical parameter dictates pipe structural design, machine selection, and working shaft layout, while governing soil stability and construction safety. Insufficient jacking force slows the advancement rate, whereas excessive force induces compressive stresses that can exceed the pipe's ultimate bearing capacity, leading to structural failure. Therefore, accurate jacking force prediction is paramount for ensuring construction safety and efficiency.

© The Author(s) 2026
H. Wu et al. (eds.), *Proceedings of the 2026 3rd International Conference on Civil Engineering Structures and Concrete Materials (CESCM 2026)*, Advances in Engineering Research 312,
https://doi.org/10.2991/978-94-6239-865-8_9

Numerous studies have investigated jacking force mechanics and prediction. Staheli[3] modified Terzaghi's arching theory to formulate jacking forces based on direct shear tests evaluating pipe-soil friction. Xu et al. [4] proposed and validated a frictional resistance model for rectangular pipe jacking by considering actual pipe-soil contact and slurry pressure counteraction. Mei et al. [5] further subdivided and verified the slurry lubrication process into progressive and full-effect stages. For rock strata, Xu et al. [6] investigated face resistance based on the rock-breaking mechanism. Concurrently, the finite element method (FEM) is widely adopted to evaluate the impacts of slurry properties [7], geometric boundary constraints [8], and slurry lubrication [9] on pipe stress and jacking force. Furthermore, Xu [10] derived a face resistance formula, providing a practical approach for calculating jacking forces in rock pipe jacking. Recent research has also expanded into specialized construction conditions, such as densely arranged pipe-roofs [11] and frozen ground [12], alongside advanced prediction frameworks including probabilistic observational approaches [13] and machine learning models (e.g., PSO-BPNN and PSO-SVR) [14].

Current methods for investigating jacking forces encompass laboratory testing, field monitoring, theoretical analysis, and numerical simulation [15-17]. Existing studies often neglect soft-over-hard composite strata and rely on assumed uniform friction coefficients. To address this, the specific novelty of this work is a field-calibrated 3D FEM framework. By deriving stage-specific friction coefficients directly from in-situ strain monitoring, our model overcomes the limitations of empirical methods (e.g., Staheli's model) in complex stratum transitions, providing high-fidelity jacking force predictions for highly variable geological conditions.

2 Project Profile

This study investigates a reinforced concrete pipe jacking operation for a 1,115 m pressureless tunnel beneath the Jiaoliu River, part of the Chaor River-Liaoning water diversion project in Inner Mongolia. The linear, northeast-southwest alignment comprises an expanded chamber, a 940 m single-drive pipe jacking segment, and a drill-and-blast section. The jacking segment features a maximum cover depth of 26 m and a longitudinal gradient of 1:1100.

The geological profile is characterized by highly variable, soft-over-hard mixed ground conditions (Figure 1). The stratigraphy predominantly consists of muddy gravel, tuff and granite. The alignment primarily traverses completely weathered muddy gravel and bedrock, with localized moderately weathered rock intrusions. This pronounced stiffness disparity in the composite strata-specifically, muddy gravel overlying highly weathered tuff-frequently induces microtunnel boring machine (MTBM) deflection and pipe sticking at the geological interfaces.

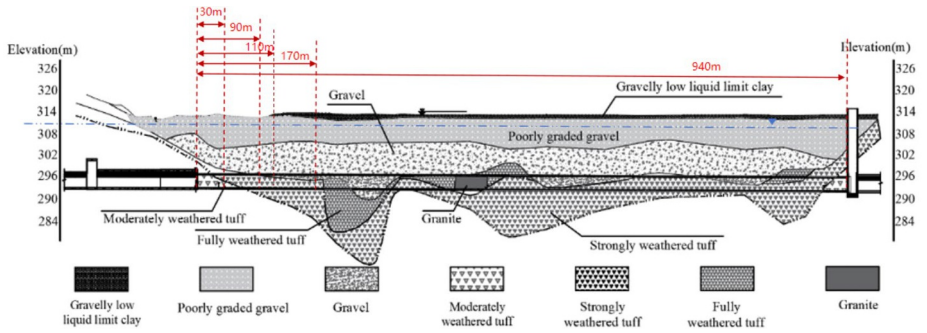


Fig. 1. Geological conditions of the Jiaoliu River pipe jacking section

The project utilizes C50 precast reinforced concrete pipes (impermeability grade P10) with an inner diameter of 3600 mm, an outer diameter of 4300 mm, and a segment length of 2500 mm. The segments are connected via flexible F-type joints sealed with wedge-shaped double rubber rings. As illustrated in Figure 2, the reinforcement cage comprises dual layers (inner and outer) of 12 mm HRB400 longitudinal and circumferential bars. The hoop spacing is 40 mm, and the longitudinal bars are distributed at 6° angular intervals. The internal and external concrete covers are 40 mm and 50 mm, respectively. For lubrication, six grouting ports are radially distributed at 60° intervals near the socket end; however, the invert port was omitted during construction, resulting in five active grouting holes per segment.

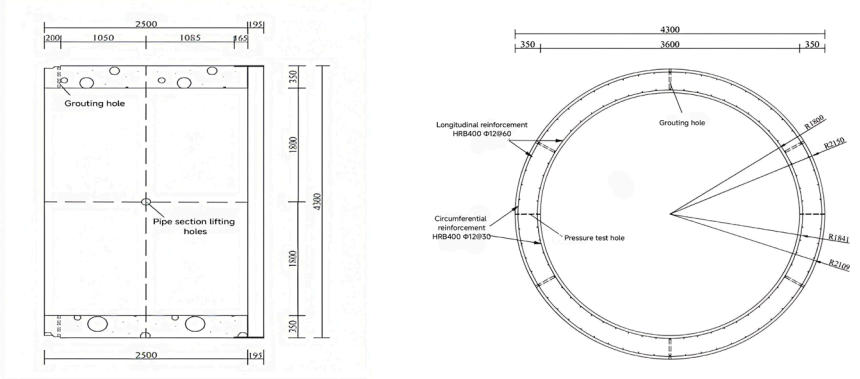


Fig. 2. Pipe Structure Schematic

3 Measurement and Analysis of Pipe Jacking Construction

3.1 On-Site Monitoring

To monitor structural safety and evaluate pipe stress states across the heterogeneous ground conditions, a comprehensive field instrumentation program was implemented on Pipe No. 38 (Figure 3). The monitoring cross-section features four measurement

points. Each point is equipped with an earth pressure cell (E-1 to E-4) and a pore water pressure transducer (P-1 to P-4) to record radial pipe-soil contact stress and external water pressure, respectively. Additionally, axial (A-1 to A-4) and circumferential (H-1 to H-4) strain gauges were welded directly to the outer reinforcement cage to capture the structural deformation response

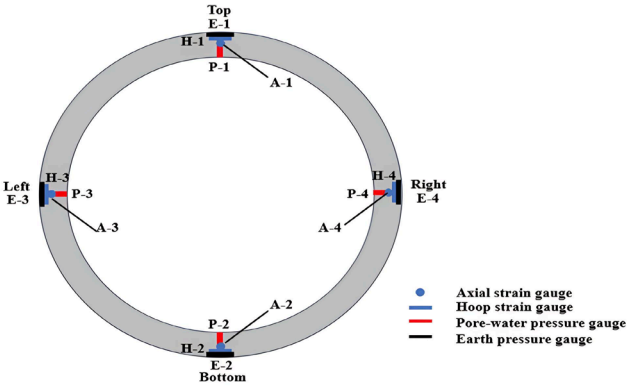


Fig. 3. Layout of monitoring sections.

3.2 Measured Analysis of Jacking Force

To eliminate measurement inaccuracies introduced by the frequent activation of intermediate jacking stations over the 940 m total drive, this study focuses on the initial 250 m section. In this interval, intermediate stations remained inactive; thus, the total jacking force strictly equaled the combined thrust of the main jacking cylinders. Field jacking forces were derived from oil pressure readings—recorded by transmitters at the main pump station—multiplied by the hydraulic cylinder area.

Figure 4 illustrates the measured jacking force versus drive length. During the initial 30 m, the alignment traverses moderately weathered tuff. Early in the drive, the jacking force increased rapidly due to a high pipe-soil friction coefficient, exacerbated by slurry loss into rock fissures before a continuous mud annulus could form. As advancement progressed, a stable mud sleeve developed, transitioning the contact mechanism from pipe-soil to pipe-slurry friction. This significantly reduced the friction coefficient, decelerating the force growth and causing localized force reductions. Between 30 m and 90 m, the machine transitioned into highly weathered tuff, with the jacking force stabilizing around 15,000 kN.

At 90 m, the alignment entered a mixed face of highly and fully weathered tuff. The loose, unstable nature of the fully weathered tuff elevated both face resistance and circumferential friction, causing a sharp force increase to approximately 21,000 kN. At 110 m, the microtunnel boring machine (MTBM) encountered the soft-over-hard composite stratum (muddy gravel over highly weathered tuff). While the muddy gravel slightly increased face resistance, its high permeability and fluidity drastically reduced peripheral friction, resulting in a sudden drop in the total jacking force. Re-entering the

highly weathered tuff at 170 m, the force surged before stabilizing, showing a 37.03% average increase compared to the preceding mixed stratum.

Throughout the entire jacking process, the measured force exhibits continuous fluctuations. These are primarily attributed to the thixotropic nature of the bentonite slurry and the repeated loading-unloading cycles required for pipe splicing; the static friction required to restart the drive consistently exceeds the dynamic sliding friction during continuous advancement.

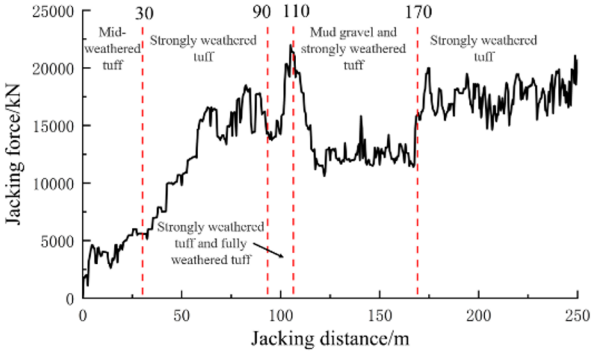


Fig. 4. Variation of measured jacking force with jacking distance curve.

3.3 Measured Analysis of Face Resistance

Face resistance, a critical component of the total jacking force, governs excavation face stability and serves as a key indicator of microtunnel boring machine (MTBM) cutterhead wear. Figure 5 presents the field-measured face resistance versus drive length, excluding the initial 30 m due to equipment malfunction.

Between 30 m and 90 m, the MTBM advanced through highly weathered tuff, recording an average face resistance of 1.8 bar. The significant fluctuations observed in this interval are attributed to the spatial variability in the weathering degree and strength of the tuff, resulting in heterogeneous cutting conditions. At 90 m, transitioning into a mixed face of fully and highly weathered tuff, the loose nature of the fully weathered stratum caused the face resistance to increase slightly, fluctuating around 1.9 bar.

At 110 m, the machine encountered the soft-over-hard composite stratum (muddy gravel overlying highly weathered tuff). Because the muddy gravel possesses lower strength and a looser structure than the tuff, higher support pressure was required to maintain face stability. Furthermore, excavated muddy gravel tends to accumulate ahead of the cutterhead, inducing abnormal torque spikes that necessitate supplementary slurry pressure to mitigate clogging. Consequently, the face resistance in this zone peaked at 2.16 bar. Re-entering the highly weathered tuff at 170 m, the face resistance gradually decreased to an average of 1.88 bar, resuming the high-amplitude fluctuations characteristic of the 30–90 m interval.

In summary, the field data indicate that face resistance is inversely correlated with stratum competence; advancing through weaker, looser formations necessitates correspondingly higher face support pressures.

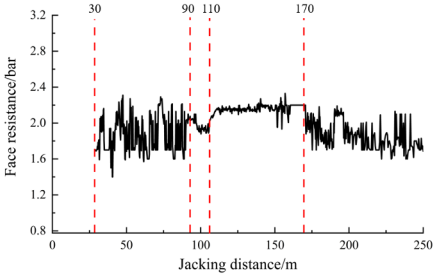


Fig. 5. Measured headway resistance variation curve with jacking distance.

3.4 Measured Inverse Friction Coefficient

In reinforced concrete pipe jacking, axial strain is primarily governed by the applied jacking force. Figure 6 illustrates the stress distribution along the pipe cross-section. Based on the principle of force equilibrium, the difference between the internal axial force of any given pipe segment and the microtunnel boring machine (MTBM) face resistance equals the cumulative circumferential frictional resistance acting along the intervening pipe string. Consequently, for the NO.i pipe segment, the relationship between the pipe-soil interface friction coefficient and the internal axial force is expressed as:

$$F_i - N = E\bar{\varepsilon_i}A - N = \mu F_c L \tag{1}$$

Where: i represents the No.i pipe. F_i is the resultant force of the axial internal force of the No.i pipe; N is the face resistance of the microtunnel boring machine; $\bar{\varepsilon_i}$ is the average axial strain of the No.i pipe; E is the average elastic modulus of reinforced concrete pipe, and is 35879.03MPa based on the actual reinforcement ratio; A refers to the cross-sectional area of the pipe, which is 4.34m^2 based on the size of the pipe; μ denotes the interface friction coefficient at the pipe exterior–soil contact; F_c is the contact pressure between pipe wall and soil; L is the jacking distance;

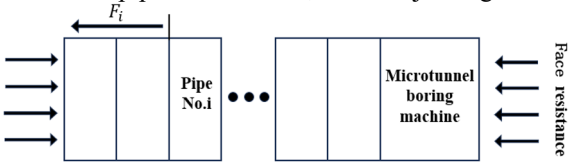


Fig. 6. Schematic diagram of pipe forces.

When the microtunnel boring machine jacked to 250m, the 38# pipe was 155m away from the cave door, and there was no monitoring data in the first 30m at the initial stage of jacking due to equipment failure, so only the data of the 38# pipe traversing the stratum of 30-155m were obtained. In view of the short distance between fully weathered tuff and strongly weathered tuff mixed strata, and the monitoring data is not much different from the strongly weathered tuff strata in the whole section, in order to facilitate the calculation, the strata within the range of 30-110m are regarded as the strongly

weathered tuff strata in the whole section, and the average on-face resistance is taken to be 1.83bar.F_c According to the monitoring data of soil pressure around the pipe, the average values of 30-110m and 110-155m are 221.78kPa and 196.15kPa respectively, and the average axial compressive strain of 38# pipe when jacking up to 30m and 110m are 87.1με and 56.67με, respectively, and the corresponding parameter is substituted into Equal (1) to calculate the frictional coefficients of the pipe-soil in the different strata. The calculation results of the formula are presented in Table 1. It is found that the pipe-soil friction coefficient in the composite layer of mud gravel and strongly weathered tuff is reduced by 14.8% compared with that in the strongly weathered tuff in the whole section, which is due to the composition and shape of the mud gravel particles are different and more heterogeneous, and this inhomogeneity leads to the increase of relative mobility between particles of the soil body under the action of stress, which then reduces the friction between the contact surfaces of the pipe-soil.

Table 1. Friction coefficients by stage

Jacking position (m)	stratum (geology)	Average coefficient of friction
30-110	Strongly weathered tuff formation	0.61
110-155m	Complex formation of mud gravels and strongly weathered tuffs	0.52

4 Numerical Simulation of Pipe Jacking

4.1 Model Establishment

Based on the results of the inverse calculation of the pipe-soil friction coefficient, abaqus finite element software is used to simulate the construction process of pipe jacking, The pipe section has an outer diameter of 4.3 m, an inner diameter of 3.6 m, and a wall thickness of 0.35 m. To minimize boundary effects, the dimensions of the soil stratum model are set to 38 m in width, 46 m in height, and 280 m in length. The soil, boring machine and pipe are all classified according to the C3D8R entity unit.

The primary strata traversed by the microtunnel boring machine in the initial 250 m are depicted in Figure 7. The parameters of each layer are presented in Table 2.

Table 2. Material parameter

Soil layer structure	Thickness (m)	Cohesion(kPa)	Angle of internal friction (°)	Modulus of elasticity (MPa)	Heaviness (kN/m^3)	Poisson's ratio
Gravelly Low-liquid-limit clay	1	8.5	25	15	19.0	0.3
Poorly graded gravel	6.5	0	29.5	100	21.0	0.22
Gravel	6.5	6.5	28	125	21.0	0.31
Strongly weathered tuff	31	100	28	30000	25.5	0.35
Microtunnel boring machine	—	—	—	200000	78.5	—
Concrete pipe joints	—	—	—	35879.03	26.0	0.2

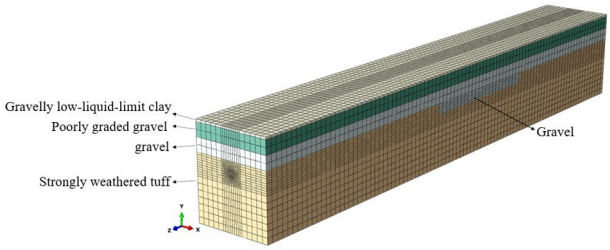


Fig. 7. Stratigraphic Material Properties Map.

Pipe-soil interactions are governed by a penalty friction formulation (Table 3). To simulate the slurry sleeve and associated ground loss, a 30-mm-thick equivalent layer is tied to the excavation boundary via shared nodes. For the soft-over-hard mixed strata, the friction coefficient of pure muddy gravel is inversely calculated as 0.43, and the displacement control method is used to simulate the excavation jacking process

Table 3. Recommended values for friction factor for concrete pipe jacking.

Material of contact surface	Frictional coefficient	Lubrication
Concrete with strongly weathered tuff	0.61	0.1-0.3
Concrete and gravel	0.43	

4.2 Analysis of Numerical Simulation Results

Simulated jacking forces were derived by multiplying the average nodal axial stress at the jacking face by the pipe cross-sectional area (4.34 m^2). These results were compared with field measurements (averaged per 2.5 m pipe segment) and analytical predictions from Staheli's model [4] across selected drive intervals (Figure 8).

As shown in Figure 8, during the 38.5-40 m stage, the simulated jacking force deviates from the measured value by 4.9%, whereas the Staheli model overestimates by 22.5% and 28.5%, respectively. At 87.5-90 m, the Staheli prediction reaches 20,109.38 kN, far exceeding both simulated and measured values, with the latter two differing by 6.1%. In the 117.5-120 m and 162.5-165 m stages (gravelly-tuff composite ground), simulated forces are 15.9% and 17.7% higher than measured ones, as field lubrication and soil deformation-absent in the simulation-reduce interface friction. At 187.5-190 m and 247.5-250 m (strongly weathered tuff), differences are 10.37% and 3.01%, respectively; the slightly higher measured value at 187.7-190 m likely reflects slurry infiltration into rock pores and rock debris, effects not modeled.

Overall, the three forces are comparable initially, but Staheli predictions become markedly larger later, while simulated and measured forces align closely throughout. This demonstrates that friction coefficients back-calculated from field data effectively capture pipe-soil interface behavior under varying strata, and their integration into numerical models substantially improves prediction accuracy. In contrast, the Staheli model, though theoretically general, cannot adequately account for complex ground

conditions with variable friction and construction disturbances. The proposed field-calibrated numerical approach thus yields more reliable jacking force predictions and offers better applicability for similar projects in complex strata.

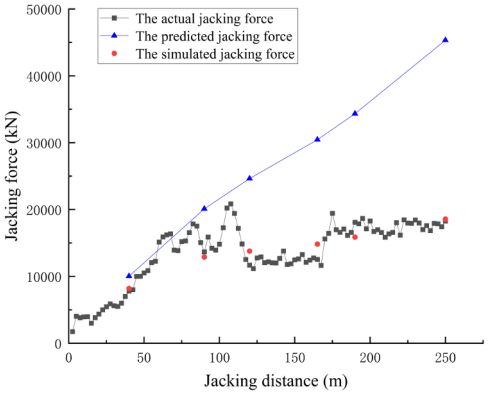


Fig. 8. Comparison between simulated jacking force and measured jacking force.

5 Conclusion

Through field tests on pipe jacking in long-distance composite strata and numerical simulation of jacking force, the following conclusions are obtained:

(1) During the process of reinforced concrete pipe jacking through composite strata, the time effect of grouting action and the influence of changes in stratum properties on the jacking force show regularity in time and space. In terms of time, due to the time effect of grouting, the jacking force in the early stage of grouting increases rapidly. When a full slurry sleeve forms around the pipe, the growth of the jacking force gradually slows down and becomes stable; in space, the jacking force is affected by the formation. Seriously, the specific manifestation occurs when the jacking force transitions from the full-section rock formation into the composite stratum of soft upper and hard lower layers, the jacking force suddenly increases, and then enters the full-section rock formation again, the jacking force increases sharply and continues to increase overall. trend.

(2) The friction coefficient calculated based on head-on resistance and axial strain is greatly affected by the properties of the formation. The friction coefficient is 14.8% lower in the composite formation of mud gravel and highly weathered tuff than in the full-section highly weathered tuff.

(3) The simulated, predicted, and measured jacking forces show consistent early-stage trends, although the predicted values are slightly higher than both the measured and simulated results. In the middle and late stages, the predicted jacking force significantly exceeds both the measured and simulated forces, while the simulated jacking force aligns closely with the measured jacking force. This indicates that the numerical simulation, using the construction site's friction coefficient, yields high accuracy, offering valuable reference for similar future projects.

References

1. Ma B.S.; Trenchless Engineering [M]. Beijing: People's Transportation Press, 2008.
2. Qi Xingbin, Zhou Li, Yin Jiangang, et al. Reinforcement design and full-scale test of high performance fiber reinforced concrete pipe jacking [J]. Journal of Underground Space and Engineering, 2025,21 (S2) 718-723 + 734.
3. Staheli K. Jacking force prediction: An interface friction approach based on pipe surface roughness[D]. Georgia Institute of Technology, 2006.
4. Xu Yong, Zhang Peng, Zeng Cong, et al. Study on calculation model of circumferential friction resistance of rectangular pipe jacking based on effective earth pressure [J]. Journal of Geotechnical Engineering, 2025,47 (9) 1967-1976.
5. Mei Jiahao, Zhang Peng, Li Shuiming, etc. Research on jacking force calculation of rectangular pipe jacking project under different mud lubrication conditions [J]. Tunnel construction (Chinese and English), 2025,45 (04): 774-781.
6. Xu T.S.; Wang L.; Liu K.X. et al. Calculation model of headway resistance of rock pipe jacking based on the rockbreaking characteristics of hob[J]. Geoscience and Technology Bulletin,2022,41(04):259-265.
7. Wang Xiangzhi. Study on preparation and drag reduction performance of new slurry for Guar gum-borax pipe jacking [D]. Anhui University of Science and Technology, 2023.
8. Xiong Y, Yan X, Wei Z, Dai F, Cai J. Study on Deformation Response Characteristics of Horizontal Main Pipeline During Vertical Jacking. Applied Sciences. 2026; 16(10):5128.
9. Ma, P., Shimada, H., Ma, B., Sasaoka, T., Hamanaka, A., Matsumoto, F., & Morita, T. (2022). SIMULATION INVESTIGATION ON THE ENGINEERING EFFECTS OF GEOMETRIC PARAMETERS IN RECTANGULAR PIPE JACKING. Paper presented at 38th Annual International No-Dig Conference and Exhibition 2022, ISTT 2022, Helsinki, Finland.
10. Xu Tianshuo, Wang Le, Liu Kaixin et al.. Calculation model of frontal resistance of rock pipe jacking based on rock breaking characteristics of disc cutter [J]. Geological Science and Technology Bulletin, 2022,41 (04).
11. Yang S, Wang M, Du J, et al. Research of jacking force of densely arranged pipe jacks process in pipe-roof pre-construction method[J]. Tunnelling and Underground Space Technology, 2020, 97: 103277.
12. Wen K.; Zeng W.; Shimada H.; et al. Numerical and theoretical study on the jacking force prediction of slurry pipe jacking traversing frozen ground[J]. Tunnelling and Underground Space Technology, 2021, 115:104076.
13. Sheil B. Prediction of microtunnelling jacking forces using a probabilistic observational approach[J]. Tunnelling and Underground Space Technology, 2021, 109: 103749.
14. Zhou H.; Huang S.; Zhang P.; et al. Prediction of jacking force using PSO-BPNN and PSO-SVR algorithm in curved pipe roof[J]. Tunnelling and Underground Space Technology, 2023, 138: 105159.
15. Zhang Y, Wu H, Chen J, et al. Study on friction characteristics at the contact interface of rock pipe jacking under complex contact modes[J]. Engineering Research Express, 2026.
16. Zhang Y.; Tao L.J.; Zhao X.; et al. Impact analysis of horizontal arrangement of first pipe jacking on thrust force of subsequent pipe jacking[J]. Journal of Southeast University (Natural Science Edition), 2021, 51(05): 762-769.
17. Zhang Yunlong, Zhang Peng, Ma Baosong, etc. Spatio-temporal distribution law and prediction model of pressure around pipe during rectangular pipe jacking construction in sand layer [J]. Chinese Journal of Geotechnical Engineering, 2023,45 (06): 1171-1179.

Open Access This chapter is licensed under the terms of the Creative Commons Attribution-NonCommercial 4.0 International License (http://creativecommons.org/licenses/by-nc/4.0/), which permits any noncommercial use, sharing, adaptation, distribution and reproduction in any medium or format, as long as you give appropriate credit to the original author(s) and the source, provide a link to the Creative Commons license and indicate if changes were made.

The images or other third party material in this chapter are included in the chapter's Creative Commons license, unless indicated otherwise in a credit line to the material. If material is not included in the chapter's Creative Commons license and your intended use is not permitted by statutory regulation or exceeds the permitted use, you will need to obtain permission directly from the copyright holder.

